Geomech. Geophys. Geo-energ. Geo-resour. (2021) 7:57
https://doi.org/10.1007/s40948-021-00247-4

ORIGINAL ARTICLE

What process causes the slowdown of pressure solution creep

Renchao Lu · Chaojie Cheng · Thomas Nagel · Harald Milsch · Hideaki Yasuhara · Olaf Kolditz · Haibing Shao

Received: 12 January 2021 / Accepted: 15 April 2021 / Published online: 15 May 2021

Abstract The slowdown of pressure solution creep has been thought to be caused by stress redistribution. This study presents a fresh view towards this creep behaviour. Basically, two rate-limiting mechanisms come into play amid pressure solution creep: (1) stress redistribution across expanding inter-granular contacts and (2) solute accumulation in the water film. Because non-hydrostatic dissolution occurs under open system conditions, solute accumulation in the water film is constrained by the ensuing solute transport process. Relying on the matter exchange across the contact surface boundary, the active processes in the voids, e.g., solute migration and deposition, affect pressure solution creep. Based upon the above, we sum up two requirements that have to be met for achieving chemical compaction equilibrium: (1) the Gibbs free energy of reaction, i.e., the driving force of non-hydrostatic dissolution process, gets depleted and (2) the concentration gradient between the water film and surrounding pore water vanishes.

Highlights

- The slowdown of pressure solution creep is a combined result of stress migration across contacts and solute accumulation in the water film.
- Matter exchange with the surroundings inhibits solute accumulation in the water film.
- This article identifies two prerequisites that need to be fulfilled for achieving chemical compaction equilibrium.

Keywords Pressure solution creep · Chemical compaction · Water-rock interaction · Non-hydrostatic dissolution

R. Lu · O. Kolditz · H. Shao (✉)
Helmholtz Centre for Environmental Research - UFZ, Leipzig, Germany
e-mail: haibing.shao@ufz.de

R. Lu
e-mail: renchao.lu@ufz.de

R. Lu · O. Kolditz
Technische Universität Dresden, Dresden, Germany

C. Cheng · H. Milsch
Helmholtz Centre Potsdam, GFZ German Research Centre for Geosciences, Potsdam, Germany

T. Nagel
Technische Universität Bergakademie Freiberg, Freiberg, Germany

T. Nagel · O. Kolditz
TUBAF-UFZ Centre for Environmental Geosciences, Freiberg, Germany

H. Yasuhara
Ehime University, Matsuyama, Japan

1 Introduction

Pressure solution creep is the dominant mechanism in marine burial diagenesis (Tada and Siever 1989; Spiers et al. 1990; Wang and Budd 2012; Gratier et al. 2009), initiated by the overburden pressure acting upon the marine sedimentary system (see Fig. 1). The ever-increasing overburden pressure densifies the loosely-packed sediments via pressure solution creep during burial. With an insight into the grain scale, the non-hydrostatic stress distributed over the inter-granular contacts (defined as the contact normal stress minus the hydrostatic pressure, c.f., Kamb (1961) and Paterson (1973)) enhances surface dissolution. As surface retreat over the contacts and hence grain repacking drain out pore water in the voids, the sediment layers are deformed to become increasingly denser and denser.

From a thermodynamic point of view to understand pressure solution creep, the open system conditions under which non-hydrostatic dissolution takes place imply that the dissolution process is not standalone but rather, accompanied by diffusive transport into the pore water outside the contacts. Therefore, the non-hydrostatic dissolution and the ensuing solute migration need to be understood as a whole constituting the mechanism of pressure solution creep.

Towards a systematic understanding of pressure solution creep, two significant scientific questions are then raised: (1) how does non-hydrostatic stress enhance mineral dissolution; and (2) what process slows down pressure solution creep over a time scale of millions of years. The former question has been well addressed by the classical thermodynamic model developed by Weyl (1959), Paterson (1973), De Boer et al. (1977), Rutter (1983), and Heidug (1995), while the latter remains to be addressed on a theoretical level. The mainstream view claims that stress redistribution causes the slowdown of creep (Revil 1999; Yasuhara et al. 2003; Gratier et al. 2013; Taron and Elsworth 2010; Bond et al. 2016; Lu et al. 2018, 2017). Stress migration across expanding contacts reduces the enhancement effect on surface dissolution so that the creep rate decreases. This plausible point of view is likely untenable or rather incomplete. If that were the case, pressure solution creep would never come to a halt as observed in the flow-through experiments where the decreasing fracture permeability is levelled

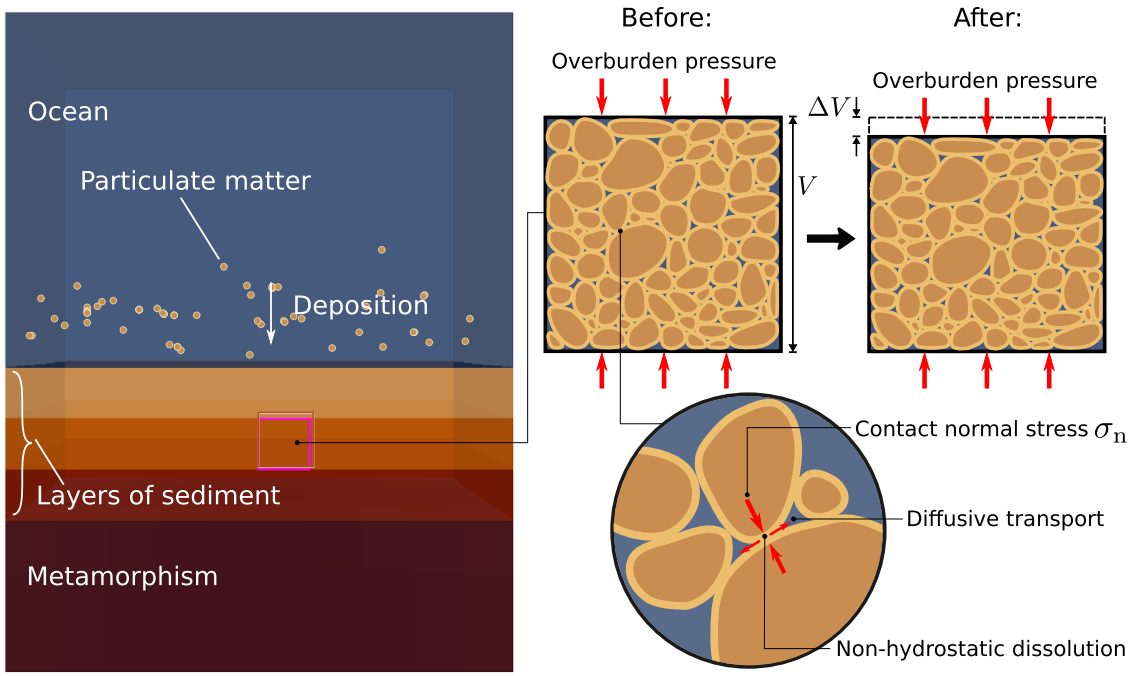

Fig. 1 Schematic representation of early diagenesis in sedimentary basins. The sediments become consolidated after undergoing the weathering of pressure solution which involves non-hydrostatic dissolution over the inter-granular contact surface, diffusive transport into the pore water outside the contacts, and possible secondary mineral precipitation

off after a long runtime (Moore et al. 1994; Niemeijer et al. 2002; Polak et al. 2003; Yasuhara et al. 2006, 2011; Okamoto et al. 2017; Cheng and Milsch 2020; Feng et al. 2020). To remedy this issue, the cessation of pressure solution creep was attributed to a reduction of the non-hydrostatic stress to the point where it is no longer sufficient to supply the required activation energy (Stephenson et al. 1992; Revil 1999; Yasuhara et al. 2003; Van Noort et al. 2008b; Taron and Elsworth 2010; Lu et al. 2017, 2018). The external work done by non-hydrostatic stress shall have been dissipated in part for crossing the activation energy barrier. The remainder of the work input gives rise to the high reactivity. Relying on the above interpretation, the established view appears convincing. However, after reviewing the derivation of the classical thermodynamic model, we find no theoretical grounds for the practice of deducting the alleged activation energy. To the authors' knowledge, the nature of the activation energy remains elusive in the context of pressure solution creep. In addition, the mineral-specific activation energy was thought to be only dependent on temperature (Stephenson et al. 1992). If so, the mineral-specific activation energy at a fixed temperature could be measured reliably. Surprisingly, we have not found any experimental study reported in this regard, which questions the plausibility of this assumption.

This study aims to explore the processes causing the slowdown of pressure solution creep further, and to remedy the confusion that has prevailed around the term activation energy in the context of pressure solution creep. For this purpose, we proceed in three steps: (1) a mathematical model of pressure solution creep is derived; (2) the rate-limiting mechanisms are identified by means of analyzing two limiting scenarios; (3) the role of solute migration is clarified.

2 Theory

2.1 Non-hydrostatic dissolution

2.1.1 High reactivity

A significant characteristic of non-hydrostatic dissolution is its high reactivity. Apparently, non-hydrostatic stress distributed over the dissolving surface is at the core of this feature. On the basis of this general understanding, the classical thermodynamic model developed by the aforementioned pioneers intrinsically interprets how non-hydrostatic stress enhances surface dissolution—the external work done by non-hydrostatic stress elevates the chemical potential of the solid phase which in turn speeds up the dissolution reaction. To formulate this dissolution enhancement mechanism, the activity of the solid under non-hydrostatic stress conditions a_s^σ [-] is presented by reference to that in the case of free-face dissolution a_s^p [-] (Paterson 1973) (see "Appendix A.1" for further details)

$$a_s^\sigma = a_s^p \exp\left(\frac{\Delta\mu_s}{RT}\right) \approx a_s^p \exp\left[\frac{(\sigma_n - p)V_m}{RT}\right], \tag{1}$$

where $\Delta\mu_s$ [J/mol] represents the mechanically-induced difference in the chemical potential of the solid phase, R [J/K/mol] is the ideal gas constant, T [K] is the temperature, σ_n [Pa] is the contact normal stress, p [Pa] is the hydrostatic pressure, and V_m [m^3/mol] is the molar volume. Note that $\sigma_n - p$ [Pa] is the bearing non-hydrostatic stress.

The contact normal stress σ_n is related to the effective stress acting on the grain σ_{eff} [Pa] and contact area ratio R_c [-] by

$$\sigma_n = \frac{\sigma_{eff}}{R_c}. \tag{2}$$

To the knowledge of the classical thermodynamic model, the non-hydrostatic stress will continue to have an effect on surface reactivity until the state of stress is fundamentally changed.

2.1.2 Attenuation characteristics

Non-hydrostatic dissolution features high reactivity, and moreover possesses attenuation characteristics as if free-face dissolution behaves. The attenuation characteristics show in the manner that the dissolution rate decreases over time, c.f., Yasuhara et al. (2006), Van Noort et al. (2008a), Yasuhara et al. (2011), and Cheng and Milsch (2020). Given these two kinetic characteristics, the normalized dissolution rate $\dot{m}$ [mol/m^2/s] (normalized mass removal rate) in this particular situation follows a more general reaction rate law where the activity of the solid is no longer implicit (Palandri and Kharaka 2004; Taron and Elsworth 2010) (see "Appendix A.2" for more information)

$$\dot{m} = k^{+} a_{\mathrm{s}}^{\sigma} \left(1 - \frac{Q}{a_{\mathrm{s}}^{\sigma} K_{\mathrm{eq}}} \right), \tag{3}$$

where k^{+} [mol/m^2/s] and K_{eq} [-] are the dissolution rate constant and equilibrium constant at hydrostatic pressure p and ambient temperature T, and Q [-] is the ion activity product.

2.2 Process description

As pressure solution creep densifies packed sediments, the inter-granular contact surface is enlarged. The extent of the growing contact surface largely depends upon the pristine grain surface morphology. Contact area growth disturbs the local sedimentary system which has been in mechanical equilibrium, triggering stress redistribution across the contact surface so as to restore equilibrium. Through such local re-equilibration processes, local stress concentrations and the resulting chemical potential of the solid phase are reduced. The decrease of the chemical potential of the solid phase inhibits the forward reaction rate, i.e., the dissolution rate, so that pressure solution creep slows down. In order to describe the overall process of pressure solution creep, the closure characteristic curve $b(R_{\mathrm{c}})$ is required for the acquisition of contact area growth from grain deformation (see Fig. 2). The closure characteristic curve is a function linking the contact area ratio R_{c} [-] to the geometric aperture b [m], and is purely determined by the pristine grain surface morphology. The creep rate is naturally parameterized by the rate of change of the geometric aperture $\dot{b}$ [m/s], equal to twice the average rate of the contact surface retreat

$$\frac{1}{2}\dot{b} = -V_{\mathrm{m}} \dot{m}. \tag{4}$$

Substituting Eq. (3) into Eq. (4), along with the closure characteristic curve $b(R_{\mathrm{c}})$, leads to an elementary equation for the process description

$$\frac{1}{2}\dot{b} = -V_{\mathrm{m}} k^{+} a_{\mathrm{s}}^{\sigma} \left(1 - \frac{Q}{a_{\mathrm{s}}^{\sigma} K_{\mathrm{eq}}} \right), \text{ with } b(R_{\mathrm{c}}). \tag{5}$$

3 Limiting-scenario analysis

3.1 Limiting scenario I

Aside from the stress redistribution, pressure solution may also result in localized thermodynamic non-equilibrium in the liquid phase due to solute accumulation in the water film. Specifically, a concentration gradient between the water film and surrounding pore water is established across the contact surface boundary. As the water film is not enclosed from all sides, solutes dissolved in the water film tend to diffuse into the pore water surrounding the contact under the driving force of the concentration gradient. The triggering of diffusion process would reduce the chemical potential of the liquid phase within the water film. With the continuous mass transfer the localized thermodynamic non-equilibrium, in terms of the concentration difference between the water film and pore water, gets relieved.

The ion activity product Q in Eq. (5) refers in particular to the chemical potential of the liquid phase remaining in the water film. This portion of chemical potential comes into play to resist contact surface retreat via the backward reaction, i.e., the precipitation reaction. The magnitude of this portion of chemical potential affects the contact surface retreat rate, depending upon the subsequent solute migration process. In a limiting scenario, we hypothesize that the solute outflux is infinitely large and instantaneous throughout the pressure solution process. This hypothesis implies in a sense that no chemical potential of the liquid phase would remain in the water film at all. Eq. (5) is thus reduced into a simplified form as

$$\frac{1}{2}\dot{b} = -V_{\mathrm{m}} k^{+} a_{\mathrm{s}}^{\sigma}, \text{ with } b(R_{\mathrm{c}}). \tag{6}$$

Eq. (6) is applied in the situation where the contact area ratio is low. A low contact area ratio not only significantly intensifies the local stress concentration over the inter-granular contact points, but also implies short diffusion pathways around the contact points and favorable conditions for solute leaching, resulting in a comparable mass out-flux against the infinitely large hypothesized in the limiting scenario. Such a situation typically occurs during the initial phase of pressure solution creep. In the illustrative example shown in Fig. 3, the yielded normal contact stress initially reaches up to 363 MPa, because the low contact area

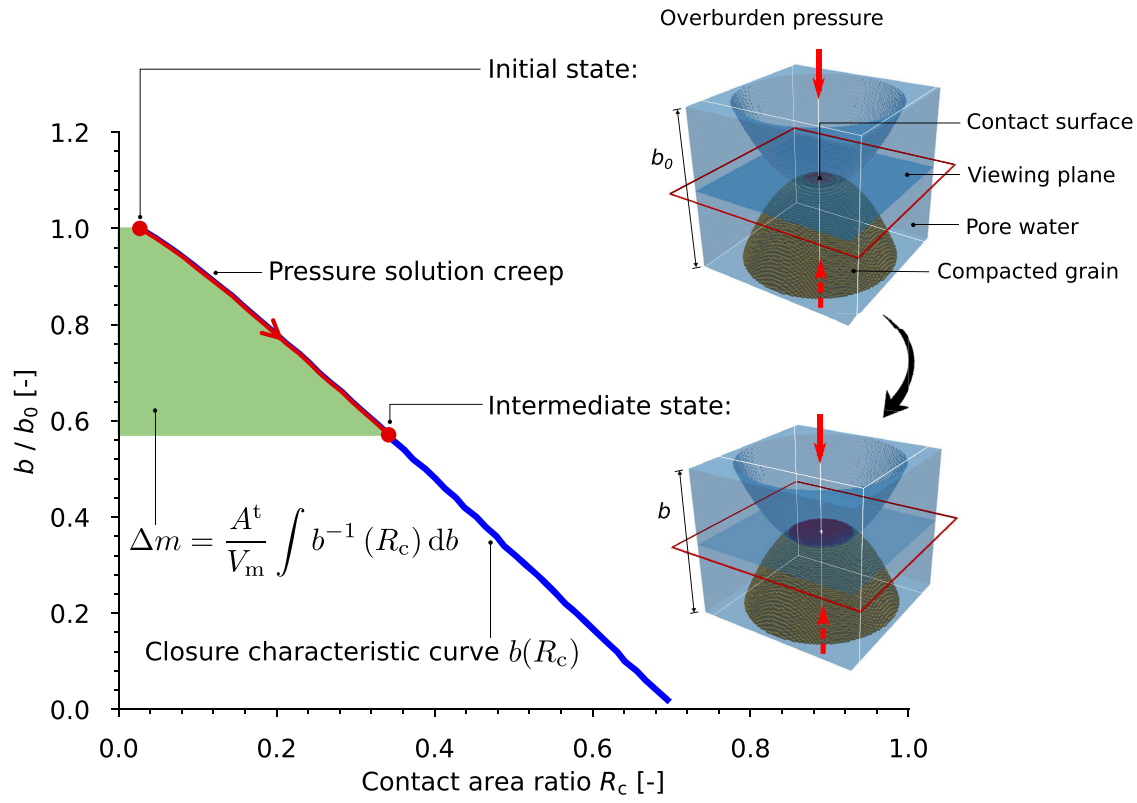

Fig. 2 A typical closure characteristic curve $b(R_c)$, constructed according to the surface morphology of the grain pair displayed on the right-hand side. The grains in pair are assumed to have a sphere-like shape in the scenario analysis. The consolidation state of the grain pair develops along the closure characteristic curve irrespective of the physiochemical process the grain pair has undergone. In the current context, pressure solution causes the consolidation state to change. The cumulative mass removal during pressure solution can be represented by the coloured area under the closure characteristic curve as $\frac{A^t}{V_m}\int b^{-1}(R_c)\mathrm{d}b$, where A^t [m^2] is the area of the chosen reference plane

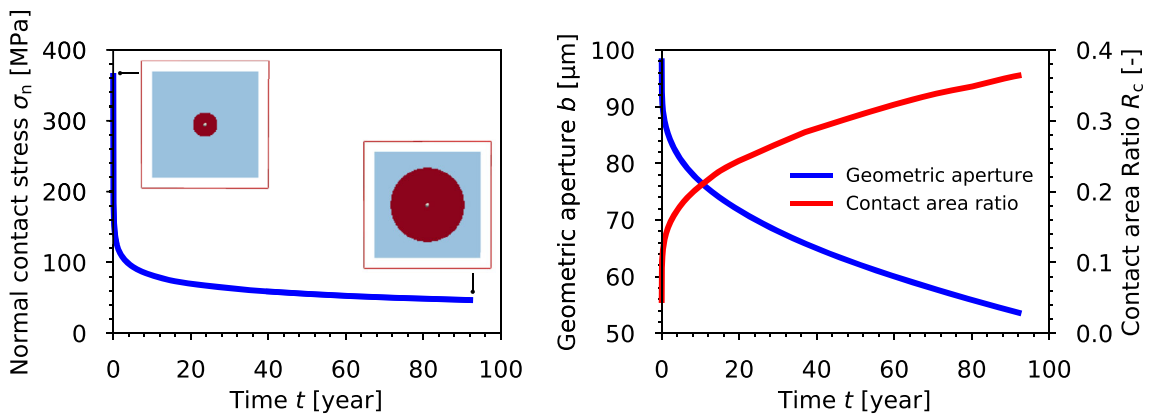

Fig. 3 Evolution of normal contact stress and geometric parameters (geometric aperture and contact area ratio) in the limiting scenario I. The parameters used for the illustrative example are: $\sigma_{\mathrm{eff}} = 17$ MPa, $p = 0.1$ MPa, $V_m = 1.0 \cdot 10^{-4}$ m^3/mol, $T = 60°$C, and $k^+ = 5.3 \cdot 10^{-12}$ mol/m^2/s. The circular contact area (coloured in red) is enlarged with the time elapsed

ratio of 4.68% amplifies the effect of stress concentration. The ultra-high applied stress exponentially raises the contact surface retreat rate by orders of magnitude, thereby leading to a sharp decrease in geometric aperture in a short period of time. As the normal contact stress is extremely sensitive to the variation of contact area in the case of low contact area ratio, sustained contact area growth will to a large extent mitigate stress concentration via its redistribution. In this example, the normal contact stress drops down rapidly below 120 MPa in response to the increasing contact area. In parallel with the stress migration across expanding contacts, the creep rate reduces in a nonlinear fashion from $4.0 \cdot 10^{-10}$ to $6 \cdot 10^{-15}$ m/s. Through such illustrative example, the nonlinear creep behavior during the initial phase can be fully understood. The interpretation being in line with the established point of view, the decease of the creep rate is dominated by stress redistribution across expanding contacts. Subsequently, the creep rate continues to decrease and is slower than in the limiting scenario; however, the dominant rate-limiting mechanism behind this further decrease may have radically changed. As argued above, the eventual cessation of the creep cannot be accounted for by stress migration across expanding contacts at all. The mechanically induced enhancement effect on surface reactivity does not vanish, despite becoming weaker as a result of stress redistribution (see Fig. 3). Eq. (6) fails to capture the creep behavior during later phases because the hypothesis of an infinitely large mass outflux is no longer justified.

3.2 Limiting scenario II

In order to figure out what other rate-limiting mechanism is involved in the long-term response, we hypothesize that mass outflux now reaches the opposite extreme—no flux across the contact surface boundary. This hypothesis forbids the transfer of the chemical potential of the liquid phase from the water film to the surrounding pore water. The chemical potential of the liquid phase within the water film thus steadily increases as the solutes dissolved in the water film accumulate. On the other hand, stress migration across the contact surface proceeds forward, decreasing the chemical potential of the solid phase. The chemical potentials of the solid phase and of the liquid phase consequently converge. Once the chemical potential difference between the solid and liquid phases, i.e., the Gibbs free energy of reaction, vanishes, pressure solution creep and densification of the packed sediments will cease. From the thermodynamic perspective, we thus ascertain two individual processes that lead to the decrease of the Gibbs free energy of reaction: (1) concentration build-up in the water film, and (2) stress migration across expanding contacts.

Let us consider the functional link between the Gibbs free energy and the extent of the reaction for illustrative purpose. In this particular scenario, we may illustrate the kinetic process of non-hydrostatic dissolution which is presumed to occur under closed system conditions alternatively by using the process-based closure characteristic curve $b(R_c, \sigma_{eff}, V_m, T, b_0, R_{c0})$ (see Figure 4)

$$\frac{b}{b_0} = \begin{cases} 1 & R_c = R_{c0} \\ \exp\left[-\frac{\sigma_{eff} V_m}{RT}\left(\frac{1}{R_{c0}} - \frac{1}{R_c}\right)\right] \frac{\frac{\sigma_{eff} V_m}{R_{c0}^2 RT}(R_c - R_{c0})}{1 - \exp\left[-\frac{\sigma_{eff} V_m}{RT}\left(\frac{1}{R_{c0}} - \frac{1}{R_c}\right)\right]} & R_{c0} < R_c \leq R_c^{eq}, \end{cases} \tag{7}$$

with the initial geometric aperture and contact area ratio b_0, R_{c0}. See Lu et al. (2017) for a detailed derivation of Eq. (7). The process-based closure characteristic curve may coincidentally be constructed from a representative grain pair of particular surface morphology that may exist in the natural system. Moreover, it illustrates the dissipation path of Gibbs free energy of reaction towards the point at which chemical equilibrium is attained under closed system conditions, i.e., situations without any matter exchange with the surroundings and under the exposure to constant overburden pressure, hydraulic pressure, and temperature. Under such conditions, the equilibrium point can be determined by solving the partial derivative of Eq. (7) with respect to R_c

$$\left.\frac{db}{dR_c}\right|_{\sigma_{eff}, T} = 0 \rightarrow R_c^{eq}. \tag{8}$$

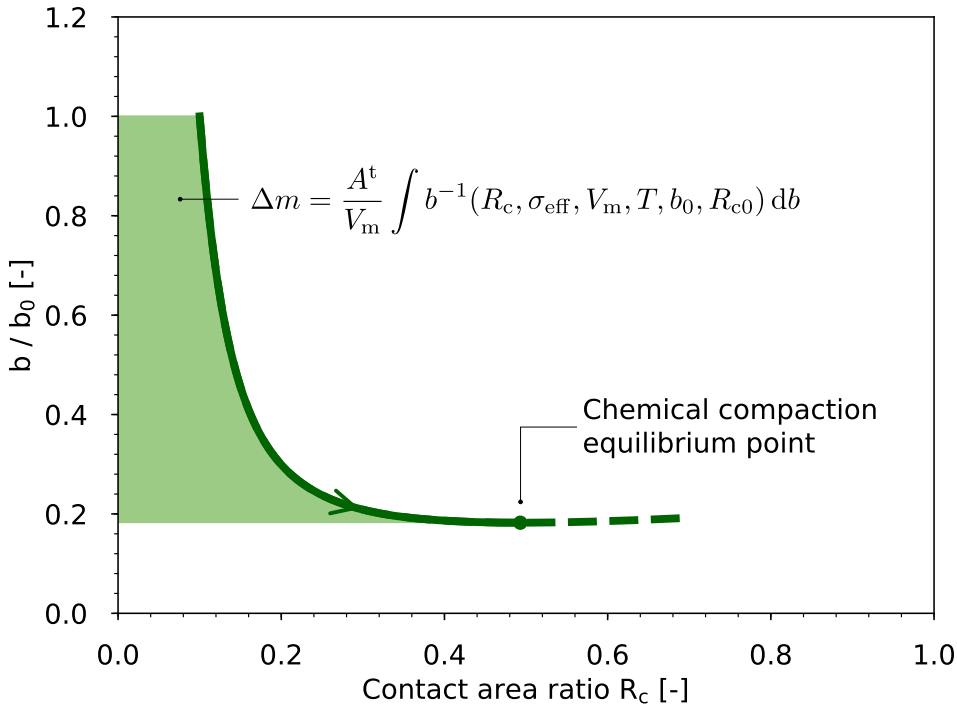

Fig. 4 A typical process-based closure characteristic curve obtained by setting $\sigma_{\mathrm{eff}} = 17$ MPa, $V_{\mathrm{m}} = 1.0 \cdot 10^{-4}$ m^3/mol, $T = 60$ °C, and $R_{\mathrm{c0}} = 0.1$. The coloured area under the process-based closure characteristic curve corresponds to the mass of the solutes dissolved into the water film by the time the chemical equilibrium is attained. Because of no mass exchange between the water film and the surrounding pore water under closed-system conditions, the chemical potential of the liquid phase within the water film increases steadily

4 Discussion

4.1 Role of solute migration

In the foregoing analysis of two limiting scenarios, we postulated the existence of either an infinitely great and instantaneous solute outflux or no mass outflux across the contact surface boundary. As a matter of fact, the actual mass outflux is situated in between the considered limiting scenarios, determined by the solute transport process. For better understanding the role of solute migration, we assume that the saturated voids outside the contact is a lower-concentration region. This assumption ensures in a sense that the matter exchange with the surroundings produces a net outflow in terms of the local sedimentary system. Driven by the concentration gradient, the solutes within the water film diffuse into the pore water so that less solutes remain in place than under closed system conditions. As long as there remains a concentration gradient across the contact surface boundary, solutes will constantly diffuse out of the water film. The continuous mass outflow, on the one hand, is unfavorable for the solute accumulation in the water film, and on the other hand, lowers the natural concentration gradient across the contact surface boundary, which in turn slows down the mass outflow. The diffusion process will not cease until the concentration gradient across the contact surface boundary absolutely vanishes. This implies that we may intervene non-hydrostatic dissolution by altering the fluid chemistry in the saturated voids. For example, we raise the solute concentration in the pore water to constrain the solute outflow from the water film which results in higher concentration levels inside the sedimentary system. As its result, the sedimentary system enables to attain chemical equilibrium earlier, i.e., at a lower contact area ratio. Alternatively, after pressure solution creep comes to a halt, we suddenly reduce the solute concentration in the pore water to re-develop a concentration gradient between the water film and surrounding pore water under which solutes resume to diffuse out into the pore water. The relaunch of diffusion process disturbs the equilibrium attained,

lowering Gibbs free energy of the system until chemical equilibrium is re-established.

As shown in Fig. 2, the area under the realistic closure characteristic curve represents the cumulative mass removal during pressure solution. In this period the solutes dissolved in the water film either remain in place or diffuse out into the pore water. By overlapping the realistic and process-based closure characteristic curves, we may further set apart the solutes that remain in place and spread out (see Fig. 5). On a graphical display, the onset of mass transfer makes the shifting of the process-based closure characteristic curve to the left. Affected by the continuous matter exchange with the surroundings, the process-based closure characteristic curve breaks down into segments (Lu et al. 2017). Mass outflux conditions how far the segments would shift towards the right (in the case of decreasing outflux) or even towards the left (in the case that the outflux is increased). The intersection point of the two closure characteristic curves represents the point at which chemical equilibrium is attained under variable open system conditions. In this way, we reconfirm two requirements that have to be met for achieving chemical compaction equilibrium: (1) the reaction Gibbs free energy for non-hydrostatic dissolution gets depleted, and (2) the concentration

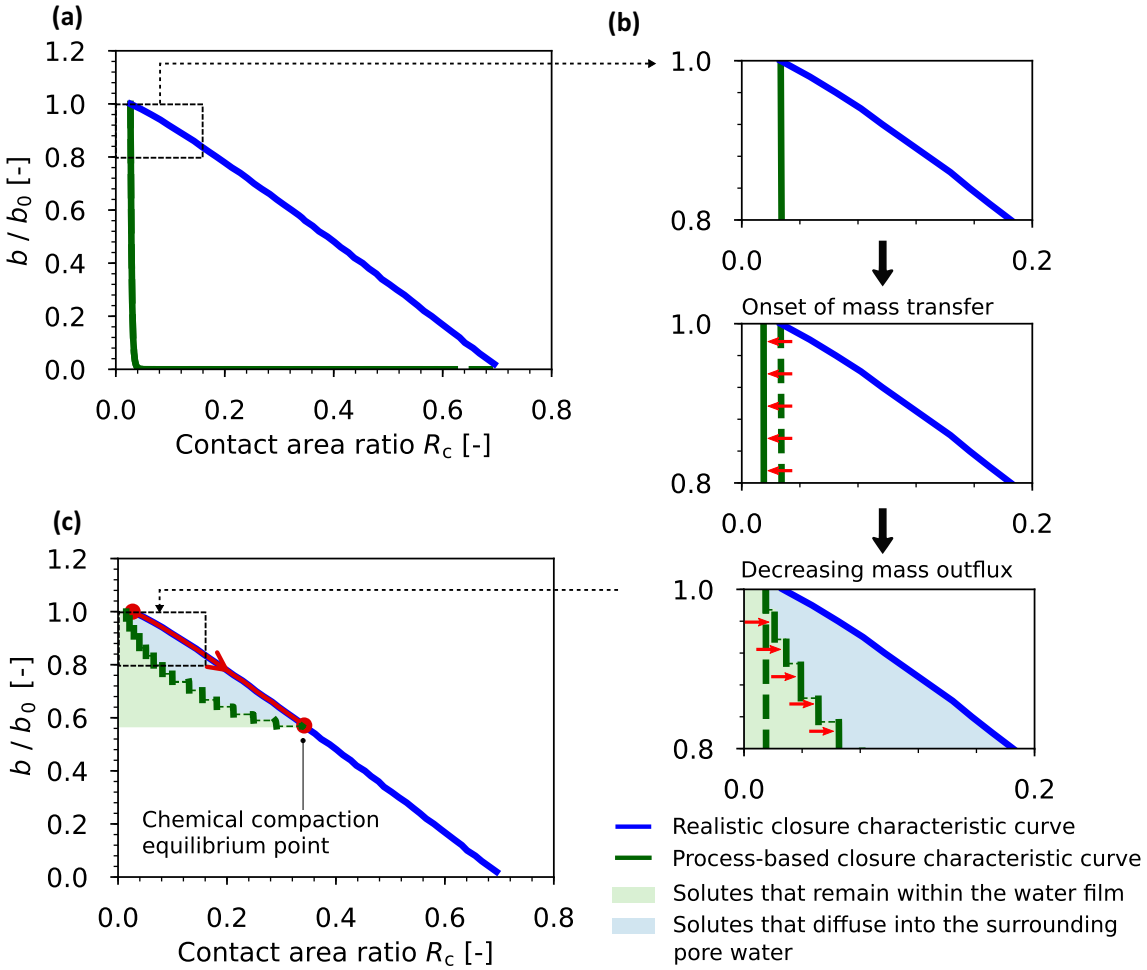

Fig. 5 Schematic diagram of the thermodynamic principle of causing the slowdown of pressure solution creep: (**a**) Overlapped closure characteristic curves. The parameters used to create the process-based closure characteristic curve are $\sigma_{\text{eff}} = 17$ MPa, $V_{\text{m}} = 1.0 \cdot 10^{-4}$ m^3/mol, $T = 60°$C, and $R_{\text{c0}} = 0.015$. (**b**) The evolution of the process-based closure characteristic curve in response to the mass exchange with the surroundings. **c**) The intersection of the two curves. The coloured areas between the realistic and process-based closure characteristic curves and under the process-based closure characteristic curve, respectively, represent the mass of the solutes that go into the surrounding pore water and that remain in the water film

gradient between the water film and the surrounding pore water goes zero.

4.2 Model limitations

In this study, we constrain ourselves to a simpler case of $\sigma_n \gg 2H\gamma$ in which the work input by normal contact stress acts as the sole driving force of dissolution enhancement (see Eq. (9) in the "Appendix A.1"). This corresponds to the situation where grain size is relatively large and the local curvature around the grain contact surfaces is small. As the grain size decreases and the local curvature increases, the interfacial free energy will linearly increase to the same magnitude as the work input by normal contact stress, i.e., $\sigma_n \approx 2H\gamma$. In that case, the effect of mean curvature can no longer be neglected, as discussed in Guével et al. (2020).

In the natural system, the packed grains may vary greatly in size, geometric shape, and surface morphology (Hodge et al. 2009; Sandeep and Senetakis 2019). Different grains in combination would have specific forms of creep rate equation, different from Eq. (4). Equation (4) holds for the case that two identical grains are ideally positioned and arranged in symmetric layout at the contact surface. In addition to the symmetry requirement, the morphology of the contact faces is simplified without the influence of intragranular surface roughness (Taron and Elsworth 2010; Liao et al. 2020). This simplification minimizes the morphological complexity but facilitates the qualitative assessments and scenario analysis in order to identify the rate-limiting mechanisms of pressure solution creep. The drawback of such simplification is that the normal contact stress is obviously underestimated and the cumulative mass removal from the grain contact surfaces is overestimated, as shown in Figs. 2, 4, and 5.

5 Conclusions

This study expounds a fresh view of the mechanisms causing the slowdown of pressure solution creep. Basically, two rate-limiting mechanisms dominate pressure solution creep: (1) stress migration across expanding contacts and (2) concentration build-up in the water film. The rate-limiting effect is achieved by reducing the reaction Gibbs free energy for non-hydrostatic dissolution. Because non-hydrostatic dissolution occurs under variable open system conditions, concentration build-up in the water film is affected by the ensuing solute migration. Relying on the matter exchange between the water film and the surrounding pore water, the active processes in the saturated voids outside the contacts, i.e., solute migration and deposition, affect pressure solution creep. On the basis of the above findings, we sum up two prior conditions for achieving chemical compaction equilibrium: (1) the reaction Gibbs free energy for non-hydrostatic dissolution gets depleted, and (2) the concentration gradient between the inside and outside of the contact vanishes in order to maintain this equilibrium.

Furthermore, it becomes clear that the activation energy in the context of pressure solution creep refers to the energy required for overcoming the chemical potential of the liquid phase remaining in the water film. The hydraulic pressure, temperature, overburden pressure, pristine grain surface morphology, and matter exchange with the surroundings all determine the activation energy.

Acknowledgements Data sharing is not applicable to this theoretical article as no new data were analyzed in this study. We acknowledge the funding support by the iCROSS-Project (Integrity of nuclear waste repository systems—cross-scale system understanding and analysis) by the Federal Ministry of Research and Education (Grant number 02NUK053E, gefördert vom BMBF) and Helmholtz Association (Helmholtz-Gemeinschaft e.V.) through the Impulse and Networking Funds (grant number SO-093). The research work is part of the new Helmholtz Research Program "Changing Earth—Sustaining our Future" Topic 8 "Georessources for the Energy Transition and a High-Tech Society".

Funding Open Access funding enabled and organized by Projekt DEAL.

Declarations

Conflict of interest The authors declare that they have no known competing financial interests or personal relationships that could have appeared to influence the work reported in this paper.

Appendix

Activity of non-hydrostatically stressed solid

In an isothermal two-phase mixture system, the chemical potential of the solid under loading conditions can be expressed as (Heidug 1995)

$$\mu_s(\sigma_n) = \mu_s^{\Theta} + \sigma_n V_m - 2H\gamma V_m, \tag{9}$$

where μ_s^{Θ} is the standard chemical potential of the solid, H [1/m] is the mean curvature, and γ [J/m^2] is the surface tension.

Taking its chemical potential under hydrostatic conditions which has the form

$$\mu_s(p) = \mu_s^{\Theta} + pV_m, \tag{10}$$

as the reference state, the stress-induced elevation in the chemical potential reads

$$\Delta\mu_s = (\sigma_n - p - 2H\gamma)V_m. \tag{11}$$

By utilizing the relation between the chemical potential and the activity

$$\mu(p,T) = \mu^{\Theta} + RT\ln a, \tag{12}$$

we may construct the activity of the stressed solid based on the reference configuration

$$a_s^{\sigma} = a_s^{p}\exp\left(\frac{\Delta\mu_s}{RT}\right) = a_s^{p}\exp\left[\frac{(\sigma_n - p - 2H\gamma)V_m}{RT}\right]. \tag{13}$$

Non-hydrostatic dissolution kinetics

Let us consider a general reversible dissolution-precipitation reaction that occurs under non-hydrostatic conditions,

$$M_s + H_2O \leftrightarrow \sum_{p=1}^{n} s_p A_p. \tag{14}$$

Given the contribution of mechanical stress to chemical affinity, the expression for Gibbs free energy of reaction is extended to

$$\Delta G = \Delta G^{\Theta} + RT\ln\prod_{p=1}^{n} a_p^{s_p} - RT\ln a_s^{\sigma}, \tag{15}$$

where ΔG^{Θ} [J/mol] is the standard free energy of reaction, and a_p [-] is the activity of a species A_p in the solution. The sign of ΔG determines the direction of the reaction. $\Delta G < 0$ indicates the reaction proceeds by spontaneous dissolution. Otherwise, if $\Delta G > 0$, mineral precipitation overwhelms dissolution. Unlike under hydrostatic conditions, the extra work input by the imposed normal stress linearly increases the deviation from the chemical equilibrium.

At equilibrium and under standard-state conditions ($a_s^{\sigma} = 1$), we have

$$\Delta G^{\Theta} = -RT\ln K_{eq}. \tag{16}$$

Inserting Eq. (16) into Eq. (15) recasts the equation into

$$\Delta G = -RT\ln K_{eq} + RT\ln\prod_{p=1}^{n} a_p^{s_p} - RT\ln a_s^{\sigma} = RT\ln\frac{Q}{a_s^{\sigma}K_{eq}}, \tag{17}$$

with the ion activity product Q [-] in place of $\prod_{p=1}^{n} a_p^{s_p}$.

The non-hydrostatic dissolution process can be described by an extended reaction rate law which links the kinetics of the reaction to the free energy of reaction

$$\dot{m} = k^{+}a_s^{\sigma}\left[1 - \exp\left(\frac{\Delta G}{RT}\right)\right] = k^{+}a_s^{\sigma}\left(1 - \frac{Q}{a_s^{\sigma}K_{eq}}\right). \tag{18}$$

References

Bond Alexander E, Bruský I, Chittenden N, Feng X-T, Kolditz O, Lang P, Renchao L, McDermott C, Neretnieks I, Pan P-Z et al (2016) Development of approaches for modelling coupled thermal-hydraulic-mechanical-chemical processes in single granite fracture experiments. Environ Earth Sci 75(19):1313

Cheng C, Milsch H (2020) Evolution of fracture aperture in quartz sandstone under hydrothermal conditions: mechanical and chemical effects. Minerals 10(8):657

De Boer RB, Nagtegaal PJC, Duyvis EM (1977) Pressure solution experiments on quartz sand. Geochim Cosmochim Acta 41(2):257–264

Feng Z, Yang Y, Niu W, Zhao Y, Wan Z, Yao Y (2020) Permeability and meso-structure evolution of coking coal subjected to long-term exposure of triaxial stresses and high pressure nitrogen. Geomech Geophys Geo-Energy Geo-Resour 6(3):1–11

Gratier J-P, Dysthe DK, Renard F (2013) The role of pressure solution creep in the ductility of the Earth's upper crust. Adv Geophys 54:47–179

Gratier J-P, Guiguet R, Renard F, Jenatton L, Bernard D (2009) A pressure solution creep law for quartz from indentation experiments. J Geophys Res Solid Earth 114:B3

Guével A, Rattez H, Veveakis E (2020) Viscous phase-field modeling for chemo-mechanical microstructural evolution: application to geomaterials and pressure solution. Int J Solids Struct 207:230–249

Heidug Wolfgang K (1995) Intergranular solid-fluid phase transformations under stress: the effect of surface forces. J Geophys Res Solid Earth 100(B4):5931–5940

Hodge R, Brasington J, Richards K (2009) Analysing laser-scanned digital terrainmodels of gravel bed surfaces: linking morphology to sediment transport processes and hydraulics. Sedimentology 56(7):2024–2043

Barclay Kamb W (1961) The thermodynamic theory of non-hydrostatically stressed solids. J Geophys Res 66(1):259–271

Liao Z, Ren M, Tang C, Zhu J (2020) A three-dimensional damage-based contact element model for simulating the interfacial behaviors of rocks and its validation and applications. Geomechan Geophys Geo-Energy Geo-Resources 6(3):1–21

Renchao L, Nagel T, Shao H, Kolditz O, Shao H (2018) Modeling of dissolution-induced permeability evolution of a granite fracture under crustal conditions. J Geophys Res Solid Earth 123(7):5609–5627

Renchao L, Wenkui HNW, Jang E, Shao H, Kolditz O, Shao H (2017) Calibration of water-granite interaction with pressure solution in a flow-through fracture under confining pressure. Environ Earth Sci 76(12):1–14

Moore Diane E, Lockner David A, Byerlee James D (1994) Reduction of permeability in granite at elevated temperatures. Science 265(5178):1558–1561

Niemeijer AR, Spiers CJ, Bos B (2002) Compaction creep of quartz sand at 400–600 C: experimen tal evidence for dissolution-controlled pressure solution. Earth Planet Sci Lett 195(3–4):261–275

Okamoto A, Tanaka H, Watanabe N, Saishu H, Tsuchiya N (2017) Fluid pocket generation in response to heterogeneous reactivity of a rock fracture under hydrothermal conditions. Geophys Res Lett 44(20):10–306

Palandri James L, Kharaka Yousif K (2004) A compilation of rate parameters of water-mineral interaction kinetics for application to geochemical modeling. Tech. rep, Geological Survey Menlo Park CA

Paterson MS (1973) Nonhydrostatic thermodynamics and its geologic applications. Rev Geophys 11(2):355–389

Polak A, Elsworth Derek, Yasuhara H, Grader AS, Halleck PM (2003) Permeability reduction of a natural fracture under net dissolution by hydrothermal fluids. Geophys Res Lett 30(20)

Revil A (1999) Pervasive pressure-solution transfer: a poro-visco-plastic model. Geophys Res Lett 26(2):255–258

Rutter EH (1983) Pressure solution in nature, theory and experiment. J Geol Soc 140(5):725–740

Sandeep CS, Senetakis K (2019) Influence of morphology on the micro-mechanical behavior of soil grain contacts. Geomechan Geophys Geo-Energy Geo-Resources 5(2):103–119

Spiers CJ, Schutjens PMTM, Brzesowsky RH, Peach CJ, Liezenberg JL, Zwart HJ (1990) Experimental determination of constitutive parameters governing creep of rocksalt by pressure solution. Geol Soc Lond Spec Publ 54(1):215–227

Stephenson LP, Plumley WJ, Palciauskas VV (1992) A model for sandstone compaction by grain inter penetration. J Sediment Res 62(1):11–22

Tada R, Siever R (1989) Pressure solution during diagenesis. Annu Rev Earth Planet Sci 17(1):89–118

Taron J, Elsworth D (2010) Constraints on compaction rate and equilibrium in the pressure solution creep of quartz aggregates and fractures: controls of aqueous concentration. J Geophys Res Solid Earth 115(B7)

Van Noort R, Spiers CJ, Pennock GM (2008a). Compaction of granular quartz under hydrothermal conditions: controlling mechanisms and grain boundary processes. J Geophys Res Solid Earth 113(B12)

Van Noort R, Visser Hendrica JM, Spiers Christopher J (2008b) Influence of grain boundary structure on dissolution controlled pressure solution and retarding effects of grain boundary healing. J Geophys Res Solid Earth 113(B3)

Wang Y, Budd David A (2012) Stress-induced chemical waves in sediment burial diagenesis. Nat Commun 3(1):1–7

Weyl Peter K (1959) Pressure solution and the force of crystallization: a phenomenological theory. J Geophys Res 64(11):2001–2025

Yasuhara H, Kinoshita N, Ohfuji H, Dae SL, Nakashima S, Kishida K (2011) Temporal alteration of fracture permeability in granite under hydrothermal conditions and its interpretation by coupled chemo-mechanical model. Appl Geochem 26(12):2074–2088

Yasuhara H, Elsworth D, Polak A (2003) A mechanistic model for compaction of granular aggregates moderated by pressure solution. J Geophys Res Solid Earth 108(B11)

Yasuhara H, Polak A, Mitani Y, Grader Abraham S, Halleck Phillip M, Elsworth D (2006) Evolution of fracture permeability through fluid-rock reaction under hydrothermal conditions. Earth Planet Sci Lett 244(1–2):186–200